6

8

10

11

12

13

14

15

17

18

26

27

28

A Robust State Estimation Framework Considering Measurement Correlations and Imperfect Synchronization

Junbo Zhao, Student Member, IEEE, Shaobu Wang, Member, IEEE, Lamine Mili, Life Fellow, IEEE, Brett Amidan, Renke Huang, Member, IEEE, and Zhenyu Huang, Fellow, IEEE

Abstract—This paper develops a robust power system state estimation framework that accounts for correlations and imperfect time synchronization of the measurements. In this framework, correlations of the measurements obtained from the supervisory control and data acquisition (SCADA) system and the phasor measurement units (PMUs) are separately calculated through the unscented transformation and a vector auto-regression (VAR) model. Specifically, the PMU measurements during the waiting period of two successive SCADA measurement scans are buffered via a VAR model whose parameters are robustly estimated using the projection statistics. The latter take into account their temporal and spatial correlations and provide the needed measurement redundancy to suppress bad data and mitigate imperfect time synchronization. In the case where the SCADA and the PMU measurements do not arrive simultaneously at the control center, yielding imperfect measurement time synchronization, either the forecasted PMU measurements or the prior SCADA measurements from the latest state estimation run are leveraged to restore system observability. Finally, a robust generalized maximum-likelihood (GM)-estimator is extended to integrate the measurement error correlations and to handle the outliers, also known as bad data. Simulation results that stem from a comprehensive comparison with other alternatives under various conditions demonstrate the benefits of the proposed framework.

Index Terms—Power system state estimation, measurement correlations, robust estimation, phasor measurement units, vector auto-regression model, bad data, generalized regression model, imperfect time synchronization.

I. INTRODUCTION

N ACCURATE and robust state estimator (SE) is essential for various important power system applications

Manuscript received August 6, 2017; revised November 16, 2017 and December 23, 2017; accepted January 1, 2018. This work was supported in part by the U.S. National Science Foundation under Grant ECCS-1711191, in part by the Advanced Scientific Computing Research Program of the U.S. Department of Energy (DOE) Office of Science, and in part by the Transmission Reliability Program of the U.S. DOE Office of Electricity (GMLC0070). Paper no. TPWRS-01209-2017. (Corresponding author: Junbo Zhao.)

- J. Zhao and L. Mili are with the Bradley Department of Electrical Computer Engineering, Virginia Polytechnic Institute and State University, Northern Virginia Center, Falls Church, VA 22043 USA (e-mail: zjunbo@vt.edu; lmili@vt.edu)
- S. Wang, B. Amidan, R. Huang, and Z. Huang are with the Pacific Northwest National Laboratory, Richland, WA 99352 USA (e-mail: shaob.wang@pnnl.gov; b.amidan@pnnl.gov; renke.huang@pnnl.gov; zhenyu.huang@pnnl.gov).
- Color versions of one or more of the figures in this paper are available online at http://ieeexplore.ieee.org.

Digital Object Identifier 10.1109/TPWRS.2018.2790390

implemented at a control center, such as optimal power flow, contingency analysis, load forecasting, to name a few. The SE aims at calculating the most likely states of a power system given a set of assumptions, which include the following [1]: 1) the measurement errors are independent and identically distributed Gaussian random variables; 2) the measurements are assumed to be taken at the same time, that is, they are synchronized; 3) the system topology and parameter values are known with good accuracy. However, violations of these assumptions occur quite often in practice. For example, investigations carried out by the authors in [2], [3] reveal that the SCADA measurements are correlated, the measurement errors do not follow a Gaussian distribution due to impulsive noise [4], [5], and the SCADA measurements may be taken at different times and hence, may be asynchronous [6].

39

41

43

45

46

47

48

49

50

51

52

56

58

62

63

65

66

70

71

72

73

74

75

To estimate the correlations of the SCADA measurements, a point estimation approach is proposed and its impact on the state estimation accuracy is investigated in [2]. This method is further extended in [3] to account for the internal correlations between PTs and CTs. However, their benefits are not thoroughly investigated in presence of PMU measurements, which are shown to improve the state estimation accuracy when integrated with the SCADA measurements [7]–[10]. Another interesting problem that deserves further investigation is the time skewness inherent in the SCADA measurements, which have a sampling rate different from that of the PMU measurements. Consequently, these two types of measurements cannot be directly combined in the state estimator. To address this problem, Yacine et al. [11]–[14] propose to buffer the PMU measurements during the waiting period of two successive SCADA measurement scans while applying a hypothesis test to choose the optimal buffer length. Then, the statistical information, namely the sample mean and the sample covariance matrix, of the buffered PMU measurements are processed together with the received SCADA measurements by the state estimator. Note that the temporal and the spatial correlations of the PMU measurements are integrated in these approaches through a non-diagonal covariance matrix. However, the correlations of the SCADA measurements are ignored. Furthermore, the SCADA and the PMU measurements are assumed to arrive simultaneously at the expected time so that a hybrid state estimator can be performed. But this assumption may not be satisfied in practice because these two types of measurements are typically collected at different times and may be

delayed due to communication issues [15], yielding imperfect time synchronization. As a result, the hybrid state estimators proposed in [7]–[14], [16]–[19] may suffer from observability problems. Finally, both measurement types can be corrupted by large errors due to instrument failures, impulsive communication noise, cyber attacks, among others. Consequently, the performances of all these estimation approaches might degrade significantly.

2

80

81

82

83

84

85

86

87

88

89

90

91

92

93

94

95

96

97

98

99

100

101

102

103 104

105

106

107

108

109 110

111

112

113

114

115

116

117

118

120

122

124

In this paper, we develop a unified robust state estimation framework to overcome the aforementioned weaknesses. The proposed framework has the following salient features:

- 1) The correlations of both the SCADA and the PMU measurements are taken into account to improve the state estimation accuracy; to this end, the unscented transformation is applied to calculate the self and the cross-correlations among the SCADA measurements while the vector autoregression (VAR) is utilized to model the temporal and the spatial correlations among the PMU measurements; the projection statistics are extended to robustly estimate the VAR parameters along with the correlation matrices, which allows us to suppress bad PMU measurements:
- 2) The impacts of imperfect time synchronization of the SCADA and the PMU measurements on the state estimation accuracy are investigated and mitigation methods are initiated:
- 3) An extension of the robust Generalized Maximumlikelihood (GM)-estimator is proposed by integrating the measurement correlations through a generalized regression model with enhanced measurement redundancy; this estimator is able to suppress the outliers in the SCADA and the PMU measurements while achieving a high statistical efficiency;
- 4) A comprehensive comparison with other alternatives under various conditions is carried out to demonstrate the benefits of the proposed framework.

The remainder of this paper is organized as follows: Section II presents the problem formulation. The proposed robust state estimation framework considering measurement correlations and imperfect time synchronization is elaborated in Section III. Numerical results are conducted and analyzed in Section IV and finally Section V concludes the paper.

II. PROBLEM FORMULATION

A. Hybrid State Estimator and Assumptions 123

For an N-bus power system, the relationship between the measurement vector $\boldsymbol{z} \in \mathbb{R}^m$ obtained from the SCADA system 125 126 and the PMUs and the state vector $\boldsymbol{x} \in \mathbb{R}^n, n = 2N-1 < m$ 127 is given by

$$z = h(x) + e, \tag{1}$$

where $h(\cdot): \mathbb{R}^n \to \mathbb{R}^m$ is a vector-valued function that relates 128 the state vector x to the measurement vector z, which con-129 tains m_s number of real and reactive power injection and flow 130 SCADA measurements along with m_p number of PMUs' volt-131 age and current phasor measurements, yielding $m = m_s + m_p$;

 $e \in \mathbb{R}^m$ denotes the measurement error vector that is assumed to follow a Gaussian distribution with zero mean and covariance matrix $\mathbf{R} \in \mathbb{R}^{m \times m}$.

135

137

139

140

141

143

144

146

147

148

149

150

152

161

170

171

177

180

181

182

184

185

To obtain the state estimates using both the SCADA and the PMU measurements, the weighted least squares criterion is usually applied [8]–[10]. This so-called hybrid state estimator provides good state estimates if the following assumptions hold true:

- 1) The correlations of the SCADA and the PMU measurements are negligible, yielding a diagonal covariance matrix R:
- 2) The SCADA and the PMU measurements arrive simultaneously so that they can be augmented together for state estimation; in other words, they are assumed to be perfectly synchronized;
- 3) The measurement error vector is assumed to follow the Gaussian distribution.

B. Problem Statement

The above three assumptions, which are usually violated in 151 real power systems, can be revised as follows:

- 1) Assumption 1: Both the SCADA and the PMU measurements are actually correlated, yielding non-diagonal covariance matrix R. This assumption can be justified on the basis of the following facts. The errors in the outputs of the Potential (PTs) and the Current Transformers (CTs) will propagate to the power injection and the power flow measurements, inducing metered values with correlated errors [2], [3]. Furthermore, the power system loads and renewable energy-based distributed generations are continuously changing, exhibiting temporal correlations. This in turn affects other generators and loads within the same geographic area, yielding spatial correlations. Due to changes in the temporally and spatially correlated loads and generations, the nodal voltage and current phasors of the system exhibit similar statistical properties, which can be easily proved using the power flow equations [20]. As a result, both the SCADA and the PMU measurement errors are correlated, yielding non-diagonal covariance matrix R;
- 2) Assumption 2: The SCADA and the PMU measurements are assumed to arrive at different times as they rely on different communication channels and time synchronization processes, yielding the following two commonly seen scenarios in real power systems: i) since the SCADA measurements are not synchronized, it is possible that the PMU measurements arrive on time while the former are delayed; ii) due to communication issues, the PMU measurements can be delayed while the SCADA measurements arrive on time [15];
- 3) Assumption 3: Both the SCADA and the PMU measurements can be corrupted by large errors due to instrument failures, impulsive communication noise, cyber attacks, etc., inducing non-Gaussian measurement noise.

Therefore, the violations of the above three assumptions can induce large biases on the final state estimates and further cause

threats to the system security operation and control. In this paper, we aim at developing a unified robust state estimation framework to overcome all these problems while achieving a high statistical efficiency.

III. THE PROPOSED ROBUST ESTIMATION FRAMEWORK

The proposed robust estimation framework includes three major blocks, namely the integration of the measurement correlations, the construction of the generalized regression model, and the robust state filtering. This framework provides a systematic way to integrate the measurement correlations and to address imperfect measurement time synchronization in the state estimator.

200 A. Estimation of the Measurement Correlations

1) Estimation of the SCADA Measurement Correlations: Let the processed measurements be the voltage magnitudes, denoted as V_i , the current magnitudes, denoted as I_i , the angle differences between the voltage and the current phasors, denoted as δ_i , the real and reactive power injections respectively denoted as P_i and Q_i , and the power flows, respectively denoted as P_{ij}^f and Q_{ij}^f . Once the measurements obtained from the PTs and the CTs are corrupted by white noises, they will be propagated to the processed measurements through the following nonlinear functions:

$$P_i = V_i I_i \cos(\delta_i), \ Q_i = V_i I_i \sin(\delta_i), \tag{2}$$

$$P_i = \sum_{j \in \mathcal{N}_i} P_{ij}^f, \ Q_i = \sum_{j \in \mathcal{N}_i} Q_{ij}^f, \tag{3}$$

which can be organized into the following functional form:

$$\boldsymbol{z}^s = \boldsymbol{f}(\boldsymbol{u}),\tag{4}$$

where $\mathbf{z}^s = [\mathbf{V}^T \ \mathbf{I}^T \ \mathbf{P}^T \ \mathbf{Q}^T \ (\mathbf{P}^f)^T \ (\mathbf{Q}^f)^T]^T \in \mathbb{R}^{m_s}$ denotes the measurement vector and $\mathbf{u} = [\mathbf{V}^T \ \mathbf{I}^T \ \boldsymbol{\delta}^T]^T \in \mathbb{R}^{n_s}$ denotes the input vector provided by the PTs and the CTs. The meter errors associated with V_i , I_i and δ_i are propagated to the errors of the calculated P_i and Q_i , inducing cross-correlations. In addition, as $Q_i = P_i \tan(\delta_i)$, P_i and Q_i are also correlated through δ_i ; the correlated P_i and Q_i will further yield correlated P_{ij}^f and Q_{ij}^f . It is assumed that the input vector is a Gaussian random variable with mean \mathbf{u} and a diagonal error covariance matrix $\mathbf{\Omega}$, whose elements represent the known measurement errors of each PT and CT.

To capture the nonlinear statistical relationships between z^s and u, we advocate the use of the unscented transformation approach [23]. Specifically, $2n_s$ sigma points are deterministically chosen so that they capture the mean and covariance of u. They are expressed as

$$\chi_i = \mathbf{u} \pm \left(\sqrt{2n_s\Omega}\right)_i,\tag{5}$$

with weights $\varpi_i=1/2n_s, i=1,...,2n_s$. Then, each sigma point is propagated through the nonlinear function $f(\cdot)$, yielding a set of transformed samples expressed as

$$\boldsymbol{l}_i = \boldsymbol{f}(\boldsymbol{\chi}_i). \tag{6}$$

Next, the transformed sample mean \hat{z}_k^s and sample covariance matrix \hat{R}_k^s at time instant k are calculated by

$$\widehat{\boldsymbol{z}}_{k}^{s} = \sum_{i=1}^{2n_{s}} \varpi_{i} \boldsymbol{l}_{i}, \quad \widehat{\boldsymbol{R}}_{k}^{s} = \sum_{i=1}^{2n_{s}} \varpi_{i} (\boldsymbol{l}_{i} - \widehat{\boldsymbol{z}}_{k}^{s}) (\boldsymbol{l}_{i} - \widehat{\boldsymbol{z}}_{k}^{s})^{T}, \quad (7)$$

where \widehat{R}_k^s is not diagonal to account for the measurement correlations.

2) Robust Estimation of the PMU Measurement Correlations: In this paper, it is assumed that the SCADA and the PMU measurements are updated every 5 s and 1/30 s, respectively. Due to different sampling rates, there exists a time skew. To address that problem, we apply a hypothesis test [11], [12] to choose the optimal buffer length of the PMUs during the waiting period of two successive SCADA measurement scans. Then, a VAR model is developed to capture the temporal and spatial correlations of the PMU measurements. According to our previous work [20], [24], the system state vector follows a first-order VAR model. Since the PMUs measure actual system states, it is anticipated that the buffered metered time series follow that model as well. Formally, we have a VAR model of first order and dimension d at time instant k expressed as

$$\mathbf{p}_k = \mathbf{\Phi}_k \mathbf{p}_{k-1} + \boldsymbol{\varepsilon}_k, \tag{8}$$

where $p_k \in \mathbb{R}^d$ denotes the buffered PMU measurement vector; $\Phi_k \in \mathbb{R}^{d \times d}$ denotes the transition matrix; $\varepsilon_k \in \mathbb{R}^d$ is assumed to be Gaussian with zero mean and covariance matrix $S_k \in \mathbb{R}^{d \times d}$, which is not necessary diagonal due to the existence of correlations. Note that the temporal and spatial correlations of the PMU measurements are reflected by the diagonal and off-diagonal elements of the matrices Φ_k and S_k , respectively.

To estimate the correlation matrix Φ_k , the least squares estimator-based Yule-Walker approach may be applied [12], [20], [25]. However, it breaks down when there are bad leverage points, which are induced by bad PMU measurement. This is due to the fact that any bad PMU measurement will show up twice in the regression matrix, namely along the row and the vertical axis, inducing a bad leverage point. To address this issue, we extend the Projection Statistics (PS) proposed in [26] to estimate Φ_k in a robust manner. Let M denote the length of the buffered measurements and $\mathbf{X} = [\mathbf{p}_{k-1},...,\mathbf{p}_{k-M+1}]^T$ $\mathbf{Y} = [\mathbf{p}_{k-2},...,\mathbf{p}_{k-M}]^T$ and $\mathbf{\tau} = [\varepsilon_{k-1},...,\varepsilon_{k-M+1}]^T$ denote the matrices that contain the PMU metered values at different time steps. We get the VAR model given by

$$X = Y\Phi_k + \tau. \tag{9}$$

Then, by applying the PS [26] to the matrix Y, we get

$$PS_{i} = \max_{\|\boldsymbol{\ell}\|=1} \frac{\left|\boldsymbol{l}_{i}^{T}\boldsymbol{\ell} - med_{j}\left(\boldsymbol{l}_{j}^{T}\boldsymbol{\ell}\right)\right|}{1.4826 \ med_{\varrho}\left|\boldsymbol{l}_{\varrho}^{T}\boldsymbol{\ell} - med_{j}\left(\boldsymbol{l}_{i}^{T}\boldsymbol{\ell}\right)\right|}, \tag{10}$$

where $i, j, \varrho = 1, 2, ..., M$. The PS of the *i*th row vector, l_i , of the matrix Y is defined as the maximum of the standardized projections of all the l_i 's on every direction ℓ that originates from the coordinatewise medians of the Y and that passes through every data point, and where the standardized projections are based on the sample median and the medianabsolute-deviation. Extensive Monte Carlo simulations reveal

289

290

291

292

293

294

295

296

297

298

299

300

301

302

303

304

305

306

307

308

309

317

318

Q1

that the PS values follow a chi-square distribution with a degree of freedom d. Thus, the weights can be calculated 278 through $\gamma_i = \min[1, \chi_{d,0.975}^2/PS_i], i = 1, ..., M$. After detect-279 ing the PMU measurements with large errors, we suppress their effects on the correlation matrix Φ_k and its estimation error 281 covariance matrix S_k as follows: 282

$$\widehat{\mathbf{\Phi}}_k = (\mathbf{Y}^T \mathbf{W}_v \mathbf{Y})^{-1} \mathbf{Y}^T \mathbf{W}_v \mathbf{X}, \tag{11}$$

$$\widehat{\boldsymbol{S}}_k = (\boldsymbol{Y}^T \boldsymbol{W}_v \boldsymbol{Y})^{-1}, \tag{12}$$

where $W_v = \text{diag}[\gamma_i]$. Substituting (11) into (8), we obtain the forecasted PMU measurement vector $\widehat{p}_{k|k-1}$ and its covariance 284 matrix $\Sigma_{k|k-1}$ at time step k via 285

$$\widehat{\boldsymbol{p}}_{k|k-1} = \widehat{\boldsymbol{\Phi}}_k \boldsymbol{p}_{k-1}, \ \widehat{\boldsymbol{\Sigma}}_{k|k-1} = \widehat{\boldsymbol{\Phi}}_k \widehat{\boldsymbol{\Sigma}}_{k-1|k-1} \widehat{\boldsymbol{\Phi}}_k^T + \widehat{\boldsymbol{S}}_k, \quad (13)$$

where $\widehat{\Sigma}_{k-1|k-1}$ is the estimation error covariance matrix at 287 time step k-1.

Remark: Note that the SCADA measurements are updated at the time instant $k + jM_p$, j = 0, 1, ..., where k is the initial time instant where both the SCADA and the PMU measurements arrive at the control center and M_p denotes the number of snapshots of the PMUs between two successive SCADA measurement scans. Since a limited number of PMUs are installed in the system, we have to use both the SCADA and the PMU measurements received at time instant k ($k + jM_p$, j = 1, ...,later on) for power system state estimation. A linear state estimator only processing PMU measurements can be performed to keep up with the PMU sampling frequency. However, due to the lack of measurement redundancy, the noise and bad data in these measurements cannot be handled effectively, yielding unreliable state estimates. In our proposed approach, instead of using them only at time instant k, we integrate all the statistical properties of the high speed PMU measurements between two successive SCADA scans through the use of a measurement buffering and a VAR model. As a result, the SCADA and the PMU measurements can be effectively combined without losing the benefit of a high sampling frequency of the latter.

B. Generalized Regression Model

Upon the arrival of the SCADA and the PMU measurements at time step k, a redundant measurement vector $\xi_k =$ 310 $[(\widehat{z}_k^s)^T \ p_k^T \ \widehat{p}_{k|k-1}^T]^T$ can be obtained by processing the two measurement sets, yielding the following measurement model:

$$\boldsymbol{\xi}_k = \boldsymbol{c}(\boldsymbol{x}_k) + \boldsymbol{v}_k; \tag{14}$$

where $c(\cdot) = [h(\cdot)^T \Gamma_k^T \Gamma_k^T]^T$; $h(\cdot)$ represents the nonlinear relationship between the SCADA measurements and the state 314 vector; Γ_k is a constant matrix that relates the linear relationship between the PMU measurements and the system state vector; Γ_k contains the susceptances and the shunt capacitances of the π -equivalent model of the lines and transformers; the covariance of the error vector v_k is diag $[\mathbf{R}_k^s \ \mathbf{R}_k^p \ \mathbf{\Sigma}_{k|k-1}] = \mathbf{L}_k \mathbf{L}_k^T;$ L_k is obtained by the Cholesky decomposition; R_k^p denotes the diagonal error covariance matrix of the received PMU measurement vector, whose diagonal elements are determined by the meter device classes of precision and the off-diagonal elements

are set to zero. By multiplying \boldsymbol{L}_k^{-1} on both sides of (14), we uncorrelate the error vector, yielding the following generalized regression model:

$$\boldsymbol{y}_k = \boldsymbol{g}(\boldsymbol{x}_k) + \boldsymbol{\eta}_k, \tag{15}$$

327

328

330

331

332

333

335

337

338

339

340

341

342

343

345

346

347

348

349

350

352

353

354

355

357

358

359

362

363

365

367

368

369

where $\mathbb{E}[\boldsymbol{\eta}_k \boldsymbol{\eta}_k^T] = \boldsymbol{I}$ is an identity matrix.

Remark: Since the SCADA measurements are not perfectly synchronized and the PMU measurements can arrive at the control center at different time instants due to communication delays or cyber attacks, the metered values, $\widehat{\boldsymbol{z}}_k^s, \boldsymbol{p}_k$ and $\widehat{\boldsymbol{p}}_{k|k-1}$, mat not arrive simultaneously at time k. To mitigate the effects of imperfect time synchronization, we present the following two strategies: i) if the PMU measurements are delayed, we will substitute them by the forecasted $\widehat{p}_{k|k-1}$, which makes the measurement vector to reduce to $\boldsymbol{y}_k = [(\widehat{\boldsymbol{z}}_k^s)^T \ \widehat{\boldsymbol{p}}_{k|k-1}^T]^T$, such that the correlations of the SCADA and the PMU measurements can still be leveraged; ii) if the SCADA measurements are delayed or lost, we propose to use the a priori state information at the latest state estimation run to restore system observability, where only the SCADA measurements are used over the area not observed by the PMUs. In this case, although the correlations of the SCADA measurements may not be well integrated, we still take into account the temporal and spatial correlations of the PMU measurements. Note that thanks to the temporal correlations of the PMUs, many historical SCADA measurements can now be updated and only a small portions of the system are affected by the imperfect time synchronization problems. Last but not the least, the enhanced measurement redundancy of the generalized regression model allows us to handle multiple bad data, which will be shown in the next section and the numerical result section.

C. Robust State Filtering

As both the SCADA and the PMU measurements can be contaminated with gross errors due to instrumental errors, impulsive communication noises, etc., this paper resorts to robust statistics [27] and advocates the use of the generalized maximum-likelihood (GM)-estimator for robust state filtering. This estimator minimizes an objective function defined as

$$J(x) = \sum_{i=1}^{m+m_p} \omega_i^2 \rho(r_{S_i}),$$
 (16)

where the time subscript k is ignored for simplicity; m denotes the total number of received SCADA and PMU measurements at the time instant k; m_p denotes the number of the buffered PMU measurements; ω_i is calculated by applying the projection statistics [26] to the Jacobian matrix $\Psi = \partial q/\partial x$ evaluated at flat voltage phasor or state vector from the previous time step. Formally, the weights of each measurement can be calculated through $\omega_i = min[1, \chi^2_{\nu, 0.975}/PS_i]$ and ν is the number of none-zero elements of the *i*th row of Ψ ; $\rho(\cdot)$ denotes the Huber convex cost function defined as

$$\rho(r_{S_i}) = \begin{cases} r_{S_i}^2/2 & \text{for } |r_{S_i}| \le \lambda \\ \lambda |r_{S_i}| - \lambda^2/2 & \text{for } |r_{S_i}| > \lambda \end{cases}, \tag{17}$$

419

421

423

425

426

427

428

429

430

431

432

434

436

437

438

442

443

448

451

452

453

459

463

464

465

466

467

468

where the parameter λ is typically set between 1.5 and 3 [27]; $r_{S_i} = r_i/s\omega_i$ denotes the standardized residual; $r_i = y_i - g_i(\widehat{\boldsymbol{x}}); s = 1.4826 \cdot b_m \cdot \text{median} \, |r_i|$ denotes the robust scale estimate and b_m denotes a correction factor [26].

The necessary condition that the minimum of (16) satisfies is given by

$$\frac{\partial J(\boldsymbol{x})}{\partial \boldsymbol{x}} = \sum_{i=1}^{m+m_p} -\frac{\boldsymbol{\alpha}_i \omega_i}{s} \psi(r_{S_i}) = \mathbf{0}, \tag{18}$$

where α_i^T is the *i*th column vector of the Jacobian matrix Ψ ; $\psi\left(r_{S_i}\right) = \partial\rho\left(r_{S_i}\right)/\partial r_{S_i}$. We multiply and divide both sides of (18) by r_{S_i} , yielding

$$\mathbf{\Psi}^T \mathbf{W} \left(\mathbf{y} - \mathbf{g}(\mathbf{x}) \right) = \mathbf{0},\tag{19}$$

379 where $q(r_{S_i}) = \psi(r_{S_i}) / r_{S_i}$ and $W = \text{diag}(q(r_{S_i}))$.

By taking the first-order Taylor series expansion of g(x) about \hat{x}^{ℓ} and using the iteratively re-weighted least square (IRLS) algorithm [27], we obtain the following iterative form:

$$\Delta \widehat{\boldsymbol{x}}^{(\ell+1)} = \left(\boldsymbol{\Psi}^T \boldsymbol{W}^{(\ell)} \boldsymbol{\Psi}\right)^{-1} \boldsymbol{\Psi}^T \boldsymbol{W}^{(\ell)} (\boldsymbol{y} - \boldsymbol{g}(\widehat{\boldsymbol{x}}^{\ell})), \quad (20)$$

where ℓ is the iteration counter. The algorithm converges if

$$\|\Delta \widehat{x}^{(\ell+1)}\| = \|\widehat{x}_k^{(\ell+1)} - \widehat{x}_k^{(\ell)}\|_{\infty} \le 10^{-3}.$$
 (21)

384 D. Evaluation of Different Alternative Methods

385

386

387

388

389

390

391

392

393

394

395

396

397

398

399

400

401

402

403

404

405

406

407

408

409

410

411

412

413

414

To demonstrate the performance of the proposed framework under various conditions, the following six different alternatives are evaluated and compared:

- Alternative 1 (A1): only the received SCADA measurements are processed and the measurement correlations are neglected, yielding a diagonal measurement error covariance matrix; this is the traditional weighted least squares estimator based on SCADA measurements;
- 2) Alternative 2 (A2): only the received SCADA measurements are processed and the measurement correlations are accounted for via the non-diagonal elements of the measurement error covariance matrix; this is the weighted least squares estimator considering the SCADA measurement correlations that is proposed in [2];
- 3) Alternative 3 (A3): the latest arriving PMU measurements and the received correlated SCADA measurements are processed; this is the widely used approach proposed in [8]–[10]; in the case where the PMU measurements are delayed, only the received correlated SCADA measurements will be processed, reducing A3 to A2; note that in that case, the covariance matrix of the PMU measurements is diagonal;
- 4) Alternative 4 (A4): the forecasted PMU measurements and the received correlated SCADA measurements are processed; in that case, both temporal and spatial correlations of the PMU measurements are considered; note that this approach is the same as the one proposed in [12], except that here the correlations of the SCADA measurements are neglected in [12]; it turns out that the ignorance of the SCADA measurement correlations yields decreased

- estimation performance as shown by the simulation results. Thus, A4 can be considered as a better version of the approach proposed in [12];
- 5) Alternative 5 (A5): the forecasted and the latest arriving PMU measurements together with the received correlated SCADA measurements are processed; in the case where the PMU measurements are delayed, only the other two types of measurements are processed, reducing A5 to A4; note that the aim of proposing A5 is to show that with the increase of the measurement redundancy provided by both the forecasted and the received latest PMU measurements and the full consideration of measurement correlations, more accurate state estimation results can be obtained compared with the approach A4;
- 6) Alternative 6 (A6): since A5 is not robust to outliers and measurement delays, we propose a robust version of it; here, both the forecasted and the latest arriving PMU measurements along with the received correlated SCADA measurements are processed by the robust state estimator; in the case where the PMU measurements are delayed, only the other two types of measurements are processed.

Note that A1 to A5 make use of the WLS estimator with the weights provided by the measurement error covariance matrices; the normalized residual-based test is utilized to detect and process outliers in the SCADA and the PMU measurements. In addition, if the SCADA or the PMU measurements are delayed or lost, the proposed mitigation strategies in Section III-B are applied (see the remark herein).

IV. NUMERICAL RESULTS

Extensive simulations are carried out on the IEEE 30-bus and the 118-bus test systems to assess the performance of each of the aforementioned alternatives. The measurement configurations of the two test systems are as follows: 1) the IEEE 30-bus system is measured by 93 SCADA measurements, including 18 pairs of active and reactive power injections, 28 of pairs power flows and voltage magnitude of Bus 1; 2) the 118-bus system has 150 pairs of SCADA measurements, including 39 pairs of injection measurements and 111 pairs of flow measurements. To simulate temporally and spatially correlated PMU measurements, the system loads are added with 2%-10% variations around their nominal values that are modelled by the $VAR_d(1)$ process. Then, a power flow calculation is executed to get the true system bus voltage and current phasors. Next, a Gaussian noise with zero mean and a standard deviation of 4×10^{-3} is added to the voltage and current phasors to realistically simulate the PMU measurements. Furthermore, a Gaussian noise with zero mean and standard deviation 10^{-2} is added to the measurements provided by the PTs and the CTs, followed by the calculations of the SCADA measurements, i.e., the real and reactive power injection and power flow measurements, and their covariance matrix through the unscented transformation. A varying percentage of system buses are randomly chosen for PMU installation. The sampling rate of the PMU measurements is 30 samples/s while the SCADA measurements are updated every 5 s. The identified VAR model is used to forecast the PMU

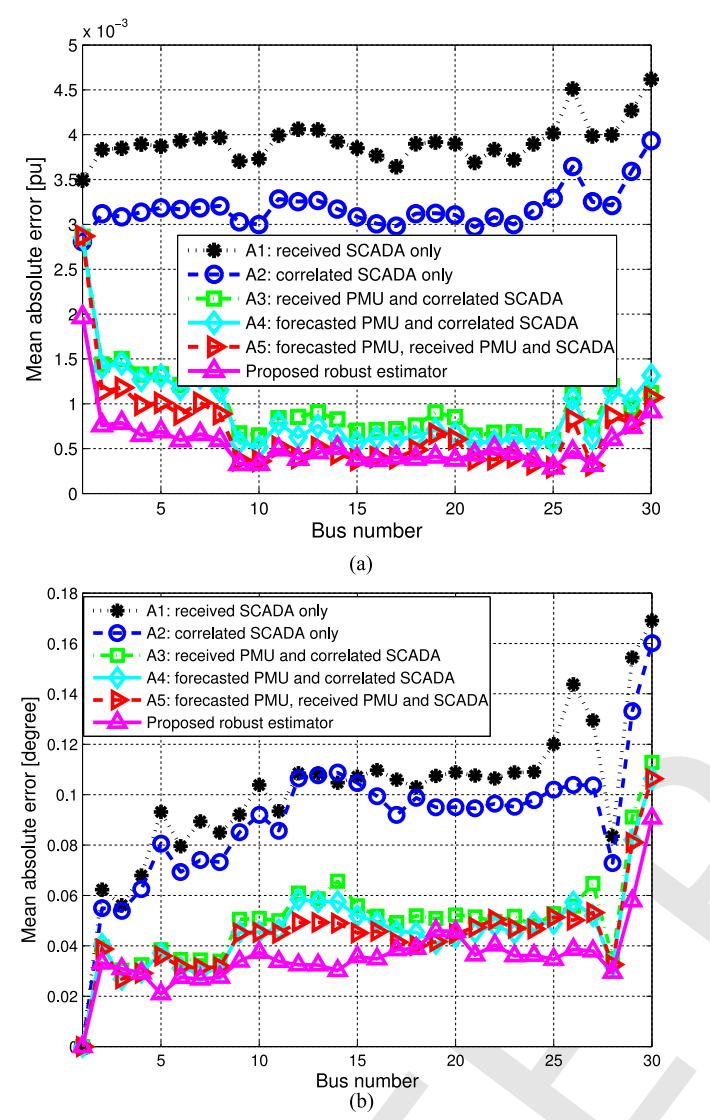


Fig. 1. MAE of the alternatives A1 through A6 for the IEEE 30-bus system, where 20% randomly chosen buses are deployed with the PMUs; (a) voltage magnitude; (b) voltage angle.

measurements as well as to calculate the full covariance matrix. The bad data detection threshold for the normalized residual test is set to 3 with 99.7% confidence level. One hundred Monte Carlo simulations are carried out to estimate the mean absolute error (MAE) of each alternative.

475 A. Ideal Operating Conditions

471

472

473

476

477

478

479

480

481

482

483

484

In this section, we evaluate the performance of each alternative under ideal operating conditions. In other words, we assume that the SCADA and the PMU measurements are synchronized, implying that they arrive simultaneously; no bad data is simulated in this case. Figs. 1 and 2 show the MAE of each alternative, for which the state estimator is applied to the IEEE 30-bus and 118-bus systems; here, 20% of randomly chosen buses are provided with PMUs. The choice of randomly deploying PMUs is justified as follows: since most of the practical systems are unobservable by PMUs, it is difficult to determine

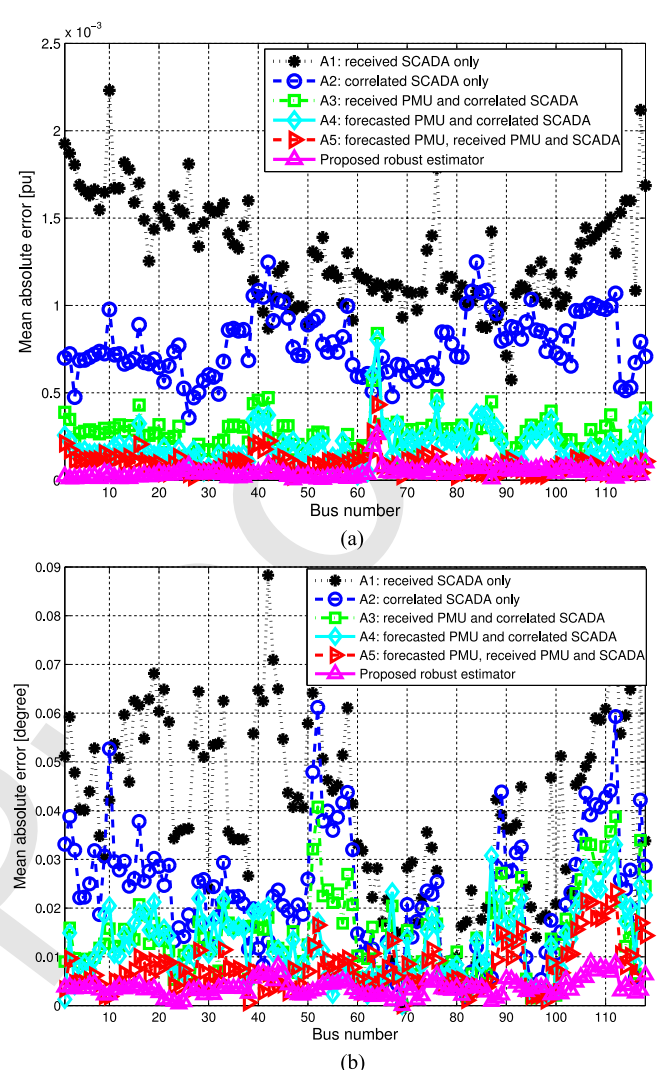


Fig. 2. MAE of the alternatives A1 through A6 for the IEEE 118-bus system, where 20% randomly chosen buses are deployed with PMUs; (a) voltage magnitude; (b) voltage angle.

487

488

490

491

492

493

494

495

496

497

498

499

500

501

503

the optimal locations of the PMUs for state estimation; thus, the random deployment is a good strategy to investigate the statistical performance of each estimator under different PMU placement scenarios. It is observed from these figures that the proposed robust estimator achieves the best performance, followed by the alternatives A5, A4, A3, A2, and finally A1, in this order. Compared with A1 and A2, we find that the integration of the SCADA measurement correlations will improve the state estimator efficiency; the inclusion of non-correlated PMU measurements can further improve the performance of A2; if the correlations of both the SCADA and the PMU measurements are taken into account, further improvement on the estimation efficiency can be achieved (see A4 and A5); compared with A3 to A5, we find that the consideration of the PMU correlations do not significantly contribute to the improvement of the state estimator efficiency, which is expected since the good accuracy of the PMU measurements is not the dominant factor that contributes to that enhancement. We find that the proposed robust state estimator used in A6 is slightly more efficient than the

TABLE I

MAE FOR THE VOLTAGE ANGLES OF THE IEEE 30-BUS SYSTEM WITH

DIFFERENT PMU PLACEMENTS

Cases	A3	A4	A5	Proposed method	
Case 1	0.092	0.0875	0.0806	0.068	
Case 2	0.0825	0.0749	0.071	0.051	
Case 3	0.052	0.042	0.032	0.014	

WLS state estimator used in A5 at most buses, and it is significantly more efficient than the latter at some buses. This is due to the fact that the system loads vary randomly, among which a few may undergo significant changes while the remaining majority change slowly. It turns out that the PMU measurements from the buses that have relative large state changes may not be well characterized by the VAR model. In that case, the projection statistics algorithm and the GM-estimator will automatically identify the PMU measurements that are outliers and will assign relatively smaller weights to them. As a result, the proposed GM-estimator is more robust and more efficient than other alternatives.

To investigate the impacts of the number of the sited PMU measurements on the estimator efficiency, we consider three cases on the IEEE 30-bus system with different percentage of buses provided with PMUs: i) Case 1: 10 percents; ii) Case 2: 20 percents, and iii) Case 3: full system observability with the minimum number of PMUs, that is, Buses 2, 3, 6, 9, 10, 12, 15, 19, 25 and 27 are provided with PMUs [21]. Note that since no PMU measurements are included in A1 and A2, the MAEs of the state estimators remain at 0.126 and 0.104, respectively for all cases. Table I shows the test results of the alternatives A3 to A6. It can be concluded from this table that, with the increased number of PMUs, the MAEs of all the considered alternatives decrease. In particular, the performance of each estimator has been significantly improved when the system is observable by PMUs. However, our proposed robust estimator in A6 still outperforms all the other alternatives in that case.

B. Impact of Imperfect Measurement Time Synchronization on the Estimation Efficiency

In Section IV-A, we have assessed the performance of each alternative when all the measurements have perfect time synchronization. Note that this assumption has been made implicitly by almost all state estimation approaches proposed in the literature that combine PMU and SCADA measurements. However, this may be violated in practical power systems because of the non-time synchronization of the SCADA measurements and because of the delays incurred by the PMU measurements due to communication problems or cyber attacks. To investigate the impacts that imperfect measurement synchronization has on the estimator efficiency, the following two scenarios are considered:

Scenario 1: at the time instant where the state estimator is executed, only SCADA measurements arrive while PMU measurements are delayed. Then, the approaches A1 and A2 are not affected and A3 reduces to A2; A5 reduces to A4; the proposed approach will be the robust version of A4.

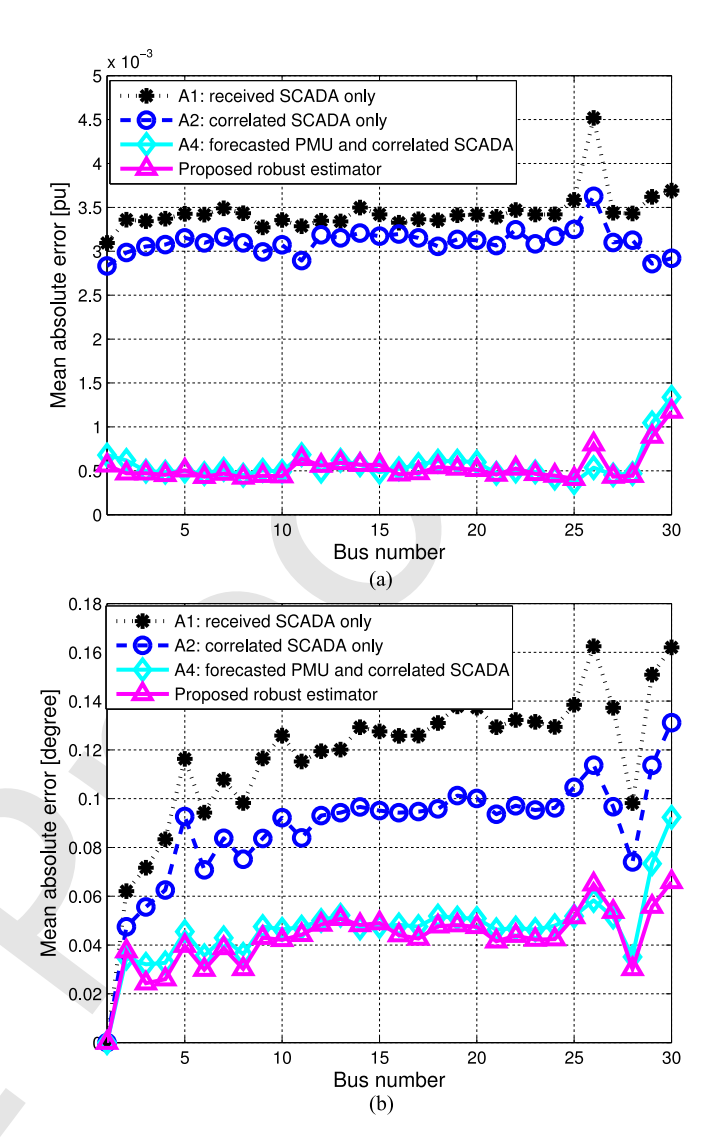


Fig. 3. Scenario 1: MAE of each alternative on the IEEE 30-bus system in presence of imperfect measurement time synchronization, where 20% randomly chosen buses are provided with PMUs; (a) voltage magnitude; (b) voltage angle.

Scenario 2: only the received and the forecasted PMU measurements are available while the SCADA measurements are delayed. Consequently, the system is partially observable. To resolve this problem, prior estimates obtained at the latest state estimation run is used. It is found that for this scenario, the results provided by the alternatives A1 and A2 are very poor, making them not suitable for state estimation. This is in contrast with the other alternatives.

Figs. 3 and 4 display the MAEs of each alternative. It is observed from Fig. 3 that, due to the loss of PMU measurements, both A4 and A6 provide increased estimation errors. However, they still outperform the SCADA-only based state estimators. When the SCADA measurements are delayed, the alternatives A3 to A6 have even larger biases on the state estimates as compared with Scenario 1. This is expected as the pseudo-measurements have to be used to restore system observability. However, these pseudo-measurements do not really reflect the current system operating conditions. As a result, the WLS state estimation used in A3 to A5 is unable to balance the trade-off

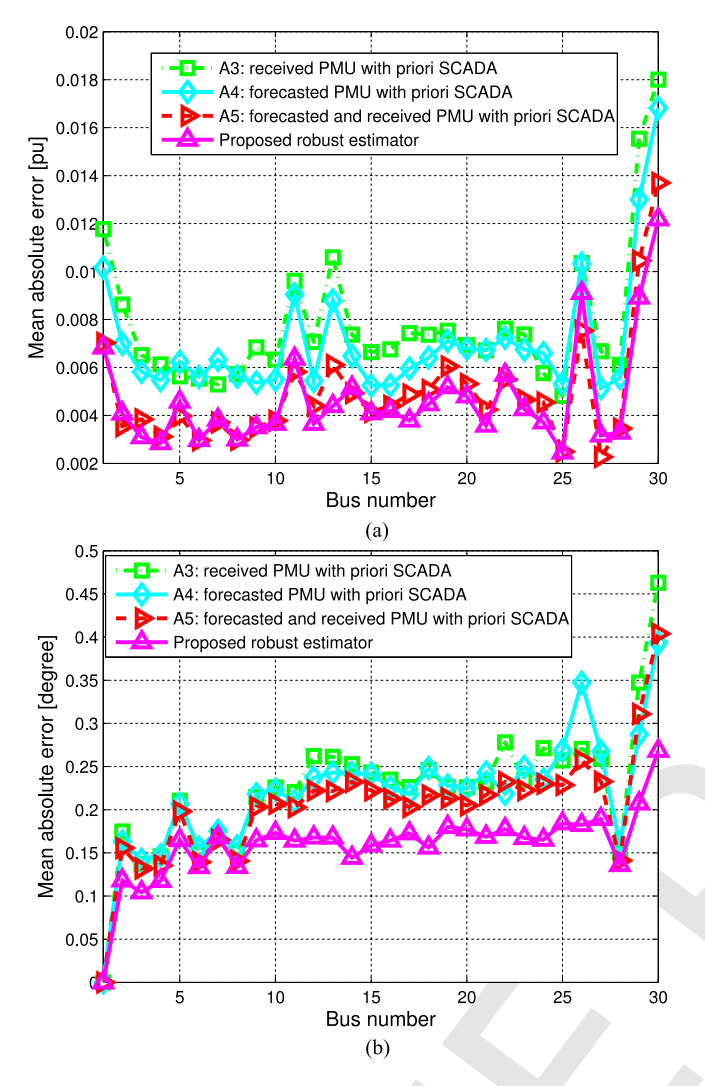


Fig. 4. Scenario 2: MAE of each alternative on the IEEE 30-bus system in presence of imperfect measurement time synchronization, where 20% randomly chosen buses are provided with PMUs; (a) voltage magnitude; (b) voltage angle.

between the current PMU measurements and the prior pseudo SCADA measurements, yielding increased estimation biases. Although our proposed robust estimator used in A6 exhibits an increased bias as well, it achieves a better balance between these two types of measurements, yielding the best performance.

575 C. Impact of Bad Data on Estimation Biases and Efficiency

Both the SCADA and PMU measurements may have gross errors due to instrument errors, or impulsive noise, or communication failures, yielding bad data. Regarding the approaches A1 to A5, the normalized measurement residual-based statistical test is applied to detect, identify, and remove the outliers, where the detection threshold is set to be 3.0 for a 99.7% confidence level. Then, the bad data processing and the state estimation are repeated until no bad data is detected. It is well-known that this approach can handle single and multiple non-interacting bad data given a good measurement redundancy and the absence of leverage points [4], [22]. To investigate the impact of the

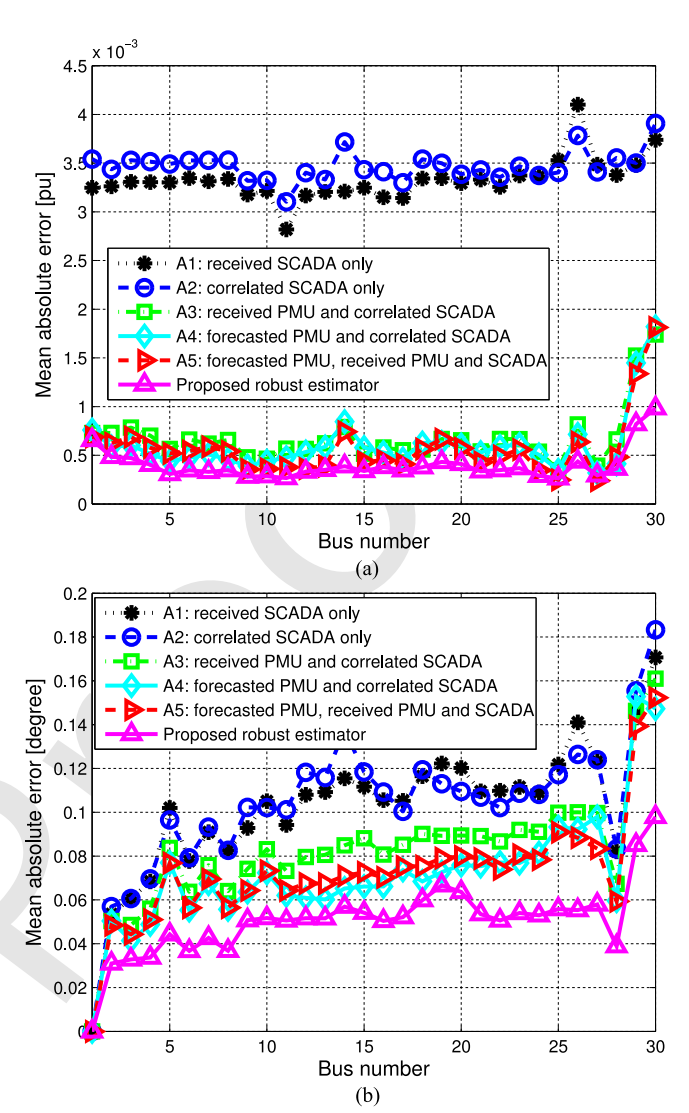


Fig. 5. Case 4: MAE of each approach on the IEEE 30-bus system in presence of bad data, where 20% randomly chosen buses are deployed with PMUs; (a) voltage magnitude; (b) voltage angle.

outliers on state estimation biases, the following two main cases are considered:

Case 4: four bad data occur, including two bad SCADA measurements P_8 and Q_8 , as well as two bad PMU measurements, θ_{12} and current flow I_{12-13} . They are assumed to be contaminated with 30% errors.

Case 5: four bad data occur, including two PMU measurements and two SCADA measurements; the latter are P_{19-20} and Q_{19-20} , which are leverage points whose magnitudes are assumed to be contaminated with 30% errors. Note that this is the case of interacting and conforming bad data. The bad PMU measurements are the same as in Case 4.

The test results for Cases 4 and 5 are depicted in Figs. 5 and 6. It can be observed from Fig. 5 that all the considered approaches are able to handle multiple non-interacting and non-conforming bad data. Compared with the cases of no bad data, the estimation errors increase slightly. Due to the enhanced measurement redundancy through the proposed generalized

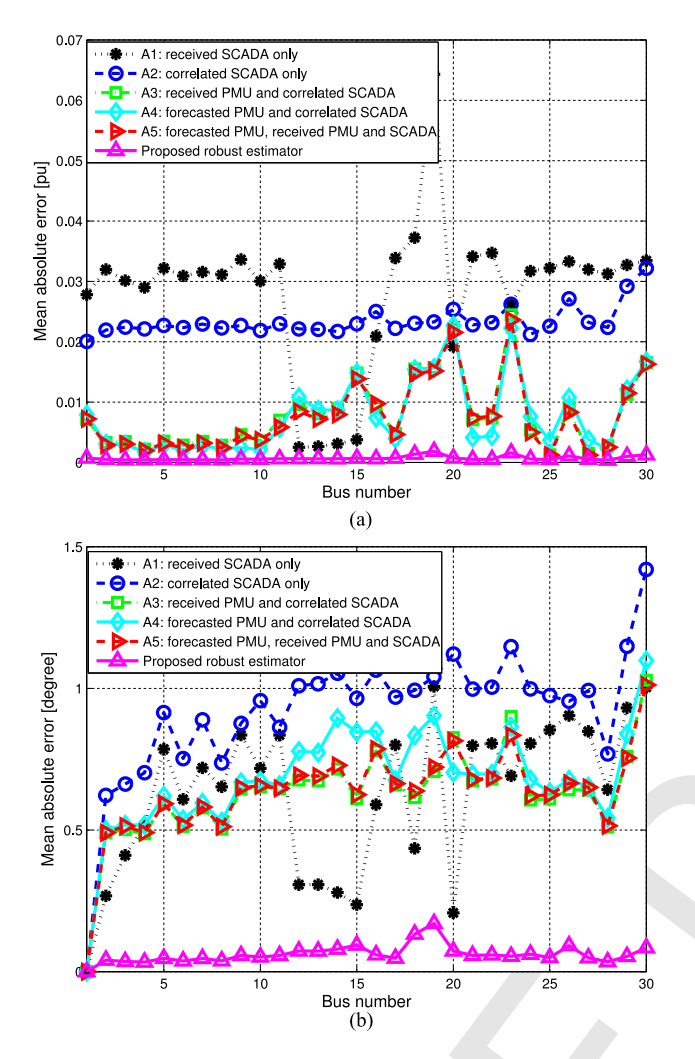


Fig. 6. Case 5: MAE of each of the six alternatives on the IEEE 30-bus system in presence of bad data, where 20% randomly chosen buses are provided with PMUs; (a) voltage magnitude; (b) voltage angle.

606

607

608

609

610

611

612

613

614

615

616

617

618

619

620

621

622

623

624

regression form and the good robustness of the GM-estimator with weights calculated using projection statistics, our robust approach significantly outperforms the other alternatives. Interestingly, the enhancement of the measurement redundancy has also improved the statistical efficiency of the traditional bad data processing method as inferred from a comparison between A5 and A1-A4. As for Case 5, it is observed that the normalized residual-based statistical test fails to identify the interacting and conforming bad data, yielding significantly biased state estimates in the alternatives A1 to A5. In fact, the weakness of the traditional chi-square test and the normalized residual single case deletion procedure when applied to clustered bad data has been demonstrated in [4]. Specifically, the normalizedresidual-based method incorrectly identifies the measurements associated with Buses 18, 15 and 14 as outliers; the latter are then removed for state estimation, yielding quite low local measurement redundancy. Specifically, due to the smearing effects caused by the outliers θ_{12} and I_{12-13} , the measurements associated with Buses 12-14 are removed by the alternatives A3 to A5, further decreasing the local measurement redundancy. In presence of interacting and conforming bad data, the

TABLE II

COMPUTATIONAL EFFICIENCY OF EACH METHOD UNDER DIFFERENT

CONDITIONS, WHERE CASE 1 IS CARRIED OUT ON THE IEEE 30-BUS SYSTEM

WHILE CASES 4–5 ARE FOR THE IEEE 118-BUS SYSTEM

Cases	A1	A2	A3	A4	A5	Proposed
Case 1	0.056 s	0.064 s	0.068 s	0.076 s	0.08 s	0.11 s
Case 4	0.34 s	0.38 s	0.48 s	0.56 s	0.86 s	0.16 s
Case 5	0.54 s	0.69 s	0.79 s	0.91 s	0.98 s	0.17 s

estimation of the SCADA measurement correlations is strongly biased, making several correct SCADA measurements associated with Buses 12–14 unreliable. As a result, the local measurement redundancies associated with A2–A5 are lower than that of A1. This justifies why A1 outperforms A2–A5 for some local buses. By contrast, the projection statistics algorithm first identifies θ_{12} and I_{12-13} as outliers and decreases their weights; then, the generalized regression model with enhanced measurement redundancy and the robustness of the GM-estimator enable our proposed robust estimator to effectively suppress bad SCADA measurements, yielding negligible estimation biases. It should be noted that the influence function of the GM-estimator [28] is bounded regardless of the interacting and conforming bad data. This justifies the effectiveness of the proposed robust estimator against various types of outliers.

D. Computational Efficiency

The computing times of the six alternatives considered for Cases 1 through 5 are displayed in Table II. Note that the results for Cases 2 and 3 are similar to those of Case 1 and therefore, are not displayed. All the tests are performed on a PC with Intel(X) Xeon(R) CPU, 3.2 GHz, 12 GB of RAM. The software platform is Matlab. From this Table, we find that in the absence of outliers, the inclusion of the measurement correlations yield higher computing times. When multiple bad data occur, the alternatives A1 to A5 become much slower than our proposed robust GM-estimator (see Cases 4 and 5). This is because the normalized residual-based test for bad data processing and reestimation is quite time consuming. By contrast, all bad data are suppressed automatically by our proposed GM-estimator and no post-processing is required, yielding improved computational efficiency. Note that in Case 5, the WLS-based residual statistical test fails to identify the correct bad data. By contrast, our robust estimator automatically suppress all the bad data while not requiring any re-estimations, yielding very good computational efficiency that is compatible with real-time applications.

V. CONCLUSION

In this paper, a robust state estimation framework is developed that integrates measurement correlations and mitigates the impacts of imperfect measurement time synchronization. The unscented transformation is applied and a vector auto-regressive (VAR) model is developed to separately integrate the correlations of the SCADA and the PMU measurements. Specifically, the PMU measurements are buffered during the waiting period of two successive SCADA measurement scans when

641

639

640

ce 647 dd 648 d- 649 dd 650 de 651 de 653 do 654 dd 655 s- 656 dr 657 de 658 d- 659 s. 660

661

663

664

666

668

678 679

680

681 682

683

684

685

686

687

688

689

690

691

692

693

694

695

696

697

698

699

700

701

702

703

704

705

706

716

717

718

719

720

721

722

724

725

726

727

728

729

731

732

733

737

738

739

740

741

742

743

744

745

746

747

748

749

750

751

752

753

754

755

756

developing the VAR model; they provide redundant measurements for imperfect time synchronization mitigation and outliers suppression. The latter is achieved via a robust GM-estimator, which also accounts for measurement correlations. Comprehensive comparison results show that our robust GM-estimator is able to significantly improve estimation efficiency while bounding the estimation bias in presence of bad data.

REFERENCES

- F. C. Schweppe and D. Rom, "Power system static state estimation, Part II: Approximate model," *IEEE Trans. Power App. Syst.*, vol. PAS–89, no. 1, pp. 125–130, Jan. 1970.
- [2] E. Caro, A. J. Conejo, and R. Minguez, "Power system state estimation considering measurement dependencies," *IEEE Trans. Power Syst.*, vol. 24, no. 4, pp. 1875–1885, Nov. 2009.
- [3] E. Caro and V. Gustavo, "Impact of transformer correlations in state estimation using the unscented transformation," *IEEE Trans. Power Syst.*, vol. 29, no. 1, pp. 368–376, Jan. 2014.
- [4] L. Mili, T. Van Cutsem, and M. Pavella, "Bad data identification methods in power system state estimation—A comparative study," *IEEE Trans. Power App. Syst.*, vol. PAS-104, no. 11, pp. 3037–3049, Nov. 1985.
- [5] J. B. Zhao, M. Netto, and L. Mili, "A robust iterated extended Kalman filter for power system dynamic state estimation," *IEEE Trans. Power* Syst., vol. 32, no. 4, pp. 3205–3216, Jul. 2017.
- [6] A. Abur and A. Gomez Exposito, Power System State Estimation: Theory and Implementation. New York, NY, USA: Marcel Dekker, 2004.
- [7] J. B. Zhao *et al.*, "Power system real-time monitoring by using PMU-based robust state estimation method," *IEEE Trans. Smart Grid*, vol. 7, no. 1, pp. 300–309, Jan. 2016.
- [8] M. Glavic and T. Van Cutsem, "Reconstructing and tracking network state from a limited number of synchrophasor measurements," *IEEE Trans. Power Syst.*, vol. 28, no. 2, pp. 1921–1929, May 2013.
- [9] A. Costa, A. Albuquerque, and D. Bez, "An estimation fusion method for including phasor measurements into power system real-time modeling," *IEEE Trans. Power Syst.*, vol. 28, no. 2, pp. 1910–1920, May 2013.
- [10] M. Zhou, V. Centeno, J. Thorp, and A. Phadke, "An alternative for including phasor measurements in state estimators," *IEEE Trans. Power Syst.*, vol. 21, no. 4, pp. 1930–1937, Nov. 2006.
- [11] Q. Zhang, Y. Chakhchoukh et al., "Impact of PMU measurement buffer length on state estimation and its optimization," *IEEE Trans. Power Syst.*, vol. 28, no. 2, pp. 1657–1665, May 2013.
- [12] Y. Chakhchoukh, V. Vittal, and G. T. Heydt, "PMU based state estimation by integrating correlation," *IEEE Trans. Power Syst.*, vol. 29, no. 2, pp. 617–626, Mar. 2014.
- [13] V. Murugesan *et al.*, "PMU data buffering for power system state estimators," *IEEE Power Energy Technol. Syst. J.*, vol. 2, no. 3, pp. 94–102, Sep. 2015.

- [14] Y. Chakhchoukh, V. Vittal, G. T. Heydt, and H. Ishii, "LTS-based robust hybrid SE integrating correlation," *IEEE Trans. Power Syst.*, vol. 32, no. 4, pp. 3127–3135, Jul. 2017.
- [15] P. Yang, Z. Tan, A. Wiesel, and A. Nehora, "Power system state estimation using PMUs with imperfect synchronization," *IEEE Trans. Power Syst.*, vol. 28, no. 4, pp. 4162–4172, Nov. 2013.
- [16] M. Gol and A. Abur, "A hybrid state estimator for systems with limited number of PMUs," *IEEE Trans. Power Syst.*, vol. 30, no. 3, pp. 1511–1517, May 2015.
- [17] G. N. Korres and N. M. Manousakis, "State estimation and bad data processing for systems including PMU and SCADA measurements," *Elect. Power Syst. Res.*, vol. 81, no. 7, pp. 1514–1524, 2011.
- [18] S. Chakrabarti E. Kyriakides, G. Ledwich, and A. Ghosh, "Inclusion of PMU current phasor measurements in a power system state estimator," *IET Gener, Transmiss., Distrib.*, vol. 4, no. 10, pp. 1104–1115, Oct. 2010.
- [19] T. Wu, C. Y. Chung, and I. Kamwa, "A fast state estimator for systems including limited number of PMUs," *IEEE Trans. Power Syst.*, vol. 32, no. 6, pp. 4329–4339, Nov. 2017.
- [20] J. B. Zhao, G. X. Zhang, Z. Dong, and M. La Scala, "Robust forecasting aided power system state estimation considering state correlations," *IEEE Trans. Smart Grid*, to be published.
- [21] T. L. Baldwin, L. Mili, M. B. Boisen, and R. Adapa, "Power system observability with minimal phasor measurement placement," *IEEE Trans. Power Syst.*, vol. 8, no. 2, pp. 707–715, May 1993.
- [22] J. B. Zhao, G. X. Zhang, M. L. Scala, and Z. Wang, "Enhanced robustness of state estimator to bad data processing through multi-innovation analysis," *IEEE Trans. Ind. Informat.*, vol. 13, no. 4, pp. 1610–1619, Aug. 2017.
- [23] S. Julier and J. Uhlmann, "A new method for the nonlinear transformation of means and covariances in filters and estimators," *IEEE Trans. Autom. Control*, vol. 45, no. 3, pp. 477–482, Mar. 2000.
- [24] M. Hassanzadeh, C. Y. Evrenosoglu, and L. Mili, "A short-term nodal voltage phasor forecasting method using temporal and spatial correlation," *IEEE Trans. Power Syst.*, vol. 31, no. 5, pp. 3881–3890, Sep. 2016.
- [25] J. B. Zhao, Z. Wang, and J. Wang, "Robust time-varying load modeling for conservation voltage reduction assessment," *IEEE Trans. Smart Grid*, to be published.
- [26] L. Mili, M. Cheniae, N. Vichare, and P. Rousseeuw, "Robust state estimation based on projection statistics," *IEEE Trans. Power Syst.*, vol. 11, no. 2, pp. 1118–1127, May 1996.
- [27] P. J. Huber, Robust Statistics. New York, NY, USA: Wiley, 1981.
- [28] J. B. Zhao and L. Mili, "Sparse state recovery vs generalized maximum-likelihood estimator of a power system," *IEEE Trans. Power Syst.*, vol. 33, no. 1, pp. 1104–1106, Jan. 2018.

Authors' photographs and biographies not available at the time of publication.

760 **Q2** 761